

# Isotropic cosmic birefringence from an oscillating axion-like field

Kai Murai<sup>1</sup>

<sup>1</sup>*Department of Physics, Tohoku University, Sendai, Miyagi 980-8578, Japan*

We propose a new mechanism for isotropic cosmic birefringence with an axion-like field that rapidly oscillates during the recombination epoch. In conventional models, the field oscillation during the recombination epoch leads to a cancellation of the birefringence effect and significantly suppresses the EB spectrum of the cosmic microwave background (CMB) polarization. By introducing an asymmetric potential to the axion, this cancellation becomes incomplete, and a substantial EB spectrum can be produced. This mechanism also results in a washout of the EE spectrum, which can be probed in future CMB observations. Our findings suggest the possibility that an axion-like field responsible for isotropic cosmic birefringence can also account for a significant fraction of dark matter.

## I. INTRODUCTION

Recently, a hint of a parity-violating signal has been reported in the polarization spectrum of the cosmic microwave background (CMB) [1–5] (see also Ref. [6] for a review). This can be explained by a rotation of the plane of the linear polarization, which is called cosmic birefringence. The reported cosmic birefringence has an isotropic rotation angle of  $\beta \sim 0.3$  deg [1–5] and has no significant frequency dependence [3, 4], which is difficult to explain within the framework of the Standard Model of particle physics [7].

As the origin of the isotropic cosmic birefringence (ICB), an axion-like particle (ALP) is widely studied [8–27]. Since the ALP is a parity-odd field coupled to photons, its temporal and spatial variations induce a parity violation in CMB. When the ALP induces cosmic birefringence, the birefringence angle,  $\beta$ , is determined only by the ALP-photon coupling and the difference of the ALP field value between the emission and observation. For appreciable ICB, the ALP field must start to oscillate after the recombination, which requires the ALP mass of  $m_\phi < \mathcal{O}(10^{-28})$  eV. Otherwise, the birefringence angle oscillates depending on the emission time of CMB photons, and the ICB angle averaged over the line of sight is highly suppressed [8, 28].

The oscillation of the birefringence angle also washes out the linear polarizations and reduces the TE and EE spectra, although they are parity-even quantities. This washout effect provides an upper bound on the ALP-photon coupling for ALP dark matter [29, 30]. Moreover, the ALP oscillation at the observer causes an oscillation in the polarization angle across the entire sky [30]. Recently, a hint of such an oscillating feature in linear polarization has been reported at the significance level of  $2.5\sigma$  by the observation of the Crab Nebula [31]. Although it is currently in tension with previous constraints [30, 32–35] when interpreted as a signal of ALP dark matter, it motivates us to explore the possibility of the oscillation of the polarization angle.

In this paper, we propose a new mechanism to cause ICB by an ALP that rapidly oscillates during the recombination epoch. We consider an ALP potential asymmet-

ric under  $\phi \leftrightarrow -\phi$ . Then, the field oscillation is also distorted, and the cancellation of the EB spectrum becomes incomplete. On the other hand, the oscillating birefringence and washout of the TE and EE spectra arise in a similar way to the conventional scenario. To validate this mechanism, we numerically evaluate the CMB polarization spectra including cosmic birefringence. We find that the ICB of  $\beta \sim 0.3$  deg can be explained without violating the constraint from the washout effect. We also provide approximate formulae to obtain the polarization spectra from the spectra without cosmic birefringence.

## II. COSMIC BIREFRINGENCE

In general, an axion-like field,  $\phi$ , is coupled with photons in a parity-violating manner. We consider a Lagrangian given by

$$\mathcal{L} = -\frac{1}{2}(\partial_\mu\phi)^2 - V(\phi) - \frac{1}{4}F_{\mu\nu}F^{\mu\nu} - \frac{1}{4}g\phi F_{\mu\nu}\tilde{F}^{\mu\nu}, \quad (1)$$

where  $V(\phi)$  is the potential for  $\phi$ ,  $F_{\mu\nu}$  is the field strength of the photon field,  $\tilde{F}^{\mu\nu}$  is its dual, and  $g$  is the ALP-photon coupling constant with mass dimension  $-1$ .

Under temporal and spatial variations of  $\phi$ , the polarization plane of linear polarization of photons rotates by an angle,  $\beta$ , given by [36–38]

$$\beta = \frac{g}{2}[\phi(t_{\text{obs}}, \mathbf{x}_{\text{obs}}) - \phi(t_{\text{emit}}, \mathbf{x}_{\text{emit}})], \quad (2)$$

where  $(t_{\text{obs}}, \mathbf{x}_{\text{obs}})$  and  $(t_{\text{emit}}, \mathbf{x}_{\text{emit}})$  are the spacetime coordinates at the observation and emission of photons, respectively. While the spatial dependence of  $\phi(t_{\text{emit}}, \mathbf{x}_{\text{emit}})$  induces anisotropic birefringence, the difference between  $\phi(t_{\text{obs}}, \mathbf{x}_{\text{obs}})$  and the spatial average of  $\phi(t_{\text{emit}}, \mathbf{x}_{\text{emit}})$  induces ICB. In the following, we focus on the homogeneous component of  $\phi(t_{\text{emit}}, \mathbf{x}_{\text{emit}})$  to obtain the isotropic component of the birefringence angle. Moreover, we are interested in the ALP that starts to oscillate before the recombination, and thus we expect  $|\phi(t_{\text{obs}}, \mathbf{x}_{\text{obs}})|$  to be negligibly small.<sup>1</sup> Then, the birefrin-

<sup>1</sup> Throughout this work, we assume that  $\phi$  oscillates around the

gence angle depends only on  $\phi$  at the emission and is given by

$$\beta(t_{\text{emit}}) \simeq -\frac{g}{2}\bar{\phi}(t_{\text{emit}}), \quad (3)$$

where we decompose  $\phi$  into its background and fluctuations as  $\phi(t, \mathbf{x}) = \bar{\phi}(t) + \delta\phi(t, \mathbf{x})$ .

To describe the effects of cosmic birefringence on the CMB polarization, we consider the Stokes parameters of linear polarization,  $Q \pm iU$ , and their Fourier transform,  ${}_{\pm 2}\Delta_P(\eta, q, \mu)$ . Here,  $\eta$  is the conformal time,  $q$  is a wavenumber vector of the Fourier mode, and  $\mu \equiv \mathbf{q} \cdot \mathbf{k}/(qk)$  is a parameter of the angle between  $\mathbf{q}$  and the photon wavenumber  $\mathbf{k}$ . The Boltzmann equation of  ${}_{\pm 2}\Delta_P(\eta, q, \mu)$  is given by [29, 39–41]

$$\begin{aligned} & {}_{\pm 2}\Delta'_P + iq\mu{}_{\pm 2}\Delta_P \\ &= \tau' \left[ -{}_{\pm 2}\Delta_P + \sqrt{\frac{6\pi}{5}} {}_{\pm 2}Y_2^0(\mu)\Pi(\eta, q) \right] \pm 2i\beta' {}_{\pm 2}\Delta_P, \end{aligned} \quad (4)$$

where the prime denotes a derivative with respect to  $\eta$ ,  ${}_{\pm 2}Y_l^m$  is the spin-2 spherical harmonics,  $\Pi$  is the polarization source term [42], and  $\tau' \equiv a(\eta)n_e(\eta)\sigma_T$  is the differential optical depth with the scale factor  $a$ , the electron number density  $n_e$ , and the Thomson scattering cross section  $\sigma_T$ . To solve the Boltzmann equation, it is convenient to expand  ${}_{\pm 2}\Delta_P$  with  ${}_{\pm 2}Y_l^0$  as

$${}_{\pm 2}\Delta_P(\eta, q, \mu) \equiv \sum_l i^{-l} \sqrt{4\pi(2l+1)} {}_{\pm 2}\Delta_{P,l}(\eta, q) {}_{\pm 2}Y_l^0(\mu). \quad (5)$$

Then, we can formally integrate the Boltzmann equation as

$$\begin{aligned} & {}_{\pm 2}\Delta_{P,l}(\eta_0, q) \\ &= -\frac{3}{4} \sqrt{\frac{(l+2)!}{(l-2)!}} \int_0^{\eta_0} d\eta \tau' e^{-\tau(\eta)} \Pi(\eta, q) \frac{j_l(x)}{x^2} e^{\pm 2i\beta(\eta)} \\ &= \int_0^{\eta_0} d\eta F(\eta, q) e^{\pm 2i\beta(\eta)}, \end{aligned} \quad (6)$$

where  $\eta_0$  is the current conformal time,  $\tau(\eta) = \int_\eta^{\eta_0} d\eta_1 \tau'(\eta_1)$ ,  $j_l$  is the spherical Bessel function, and  $x \equiv q(\eta_0 - \eta)$ . We simplified the factors other than the birefringence effect by  $F$  for simplicity of notation.

We further decompose  ${}_{\pm 2}\Delta_{P,l}$  into parity eigenstates,  $E$  and  $B$  modes, given by [42, 43]

$$\Delta_{E,l} \pm \Delta_{B,l} \equiv -{}_{\pm 2}\Delta_{P,l}(\eta_0, q). \quad (7)$$

Then, we obtain the polarization angular power spectra as

$$C_l^{XY} \equiv 4\pi \int d(\ln q) \mathcal{P}_{\mathcal{R}}(q) \Delta_{X,l}(q) \Delta_{Y,l}(q), \quad (8)$$

where  $X, Y = E$  or  $B$ , and  $\mathcal{P}_{\mathcal{R}}$  is the primordial curvature power spectrum.

## A. Isotropic Cosmic Birefringence

First, we discuss ICB induced by the time evolution of  $\bar{\phi}$ . If  $\bar{\phi}$  starts to evolve after the last scattering of the CMB photons, all photons experience the same birefringence angle,  $\beta \simeq g(\bar{\phi}(t_0) - \bar{\phi}_{\text{in}})/2$ , where  $\bar{\phi}_{\text{in}}$  is the initial value of  $\bar{\phi}$ . Then, we can factor out  $e^{\pm 2i\beta}$  in Eq. (6) and obtain

$$\Delta_{E,l} \pm \Delta_{B,l} = e^{\pm 2i\beta} (\Delta_{E,l,0} \pm \Delta_{B,l,0}), \quad (9)$$

where the subscript “0” denotes quantities without cosmic birefringence. Then, the polarization angular power spectra under cosmic birefringence are given by [39, 44, 45]

$$C_l^{EE} = C_{l,0}^{EE} \cos^2(2\beta) + C_{l,0}^{BB} \sin^2(2\beta), \quad (10)$$

$$C_l^{BB} = C_{l,0}^{EE} \sin^2(2\beta) + C_{l,0}^{BB} \cos^2(2\beta), \quad (11)$$

$$C_l^{EB} = \frac{1}{2} (C_{l,0}^{EE} - C_{l,0}^{BB}) \sin(4\beta), \quad (12)$$

where we assumed  $C_{l,0}^{EB} = 0$ . From these relations, we obtain  $C_l^{EB} \sim 0.01 C_{l,0}^{EE}$  for  $\beta \sim 0.3$  deg and  $C_{l,0}^{EE} \gg C_{l,0}^{BB}$ . As a result, by taking an appropriate value of  $g$ , the reported ICB can be explained by the ALP that evolves only after the recombination epoch. On the other hand, if  $\bar{\phi}$  evolves during the recombination epoch, these relations do not hold. In particular, if  $\bar{\phi}$  oscillates, positive and negative contributions to the EB spectrum cancel each other.

## B. Washout of CMB polarization

Next, we analytically estimate the washout effect following Ref. [30]. If the ALP rapidly oscillates during the recombination epoch,  $\beta(\eta)$  evolves much faster than  $F(\eta, q)$ . Then, we can approximate  ${}_{\pm 2}\Delta_{P,l}$  by dividing the integration over  $\eta$  into a sum of the integration over one period of the ALP oscillation:

$$\begin{aligned} {}_{\pm 2}\Delta_{P,l}(\eta_0, q) &= \sum_i \int_{\eta_i}^{\eta_i + \delta\eta_i} d\eta F(\eta, q) e^{\pm 2i\beta(\eta)} \\ &\simeq \sum_i F(\eta_i, q) \int_{\eta_i}^{\eta_i + \delta\eta_i} d\eta e^{\pm 2i\beta(\eta)}, \end{aligned} \quad (13)$$

where  $i$  is the label of the ALP oscillation, and  $\delta\eta_i$  is the oscillation period. Then, we approximate  $\beta$  in each period by

$$\beta \simeq \langle \beta \rangle_i \sin\left(2\pi \frac{\eta - \eta_i}{\delta\eta_i}\right), \quad (14)$$

---

potential minimum at  $\phi = 0$ .

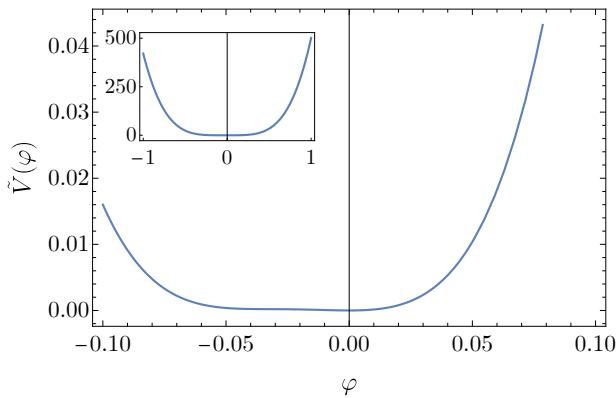


FIG. 1. Asymmetric potential  $\tilde{V}(\varphi)$  normalized as in Eq. (21). Here we use  $c_3 = 40$  and  $c_4 = 460$ .

where  $\langle\beta\rangle_i$  is the amplitude of  $\beta$  at  $\eta = \eta_i$ . Consequently, we obtain

$$\begin{aligned} \pm_2 \Delta_{P,l}(\eta_0, q) &\simeq \sum_i F(\eta_i, q) \delta\eta_i j_0(2\langle\beta\rangle_i) \\ &\simeq \int d\eta F(\eta, q) j_0(g\langle\phi\rangle(\eta)) \\ &\sim j_0(g\langle\phi\rangle_*) \pm_2 \Delta_{P,l,0}(\eta_0, q), \end{aligned} \quad (15)$$

where  $\langle\phi\rangle$  is the oscillation amplitude of the ALP field. In the last line, we made a further approximation by replacing  $j_0(g\langle\phi\rangle(\eta))$  with a representative value at  $z = z_* = 1090$ . Finally, we obtain the analytical estimate for the polarization spectra as

$$C_{l,\text{ana}}^{TE} = j_0(g\langle\phi\rangle_*) C_{l,0}^{TE}, \quad (16)$$

$$C_{l,\text{ana}}^{EE} = j_0^2(g\langle\phi\rangle_*) C_{l,0}^{EE}, \quad (17)$$

which is reduced to

$$C_{l,\text{ana}}^{TE} \simeq \left(1 - \frac{1}{4} g^2 \langle\phi\rangle_*^2\right) C_{l,0}^{TE}, \quad (18)$$

$$C_{l,\text{ana}}^{EE} \simeq \left(1 - \frac{1}{2} g^2 \langle\phi\rangle_*^2\right) C_{l,0}^{EE}, \quad (19)$$

in the limit of a small oscillation angle.

### III. NUMERICAL RESULTS

Here, we show the numerical results for the CMB polarization spectra under oscillating birefringence. Let us consider an asymmetric potential. Since this study aims to generally investigate the effects of an asymmetric potential, we adopt a simple potential given by

$$V(\phi) = \frac{m_\phi^2}{2} \phi^2 + C_3 \phi^3 + C_4 \phi^4, \quad (20)$$

where  $C_3$  and  $C_4$  are constants. Such an asymmetric potential can be realized, e.g., in the context of axion monodromy [46], where the potential is given by the sum of

a linear term and a cosine-type potential. Alternatively, a superposition of cosine potentials with different scales and phases also gives an asymmetric potential around its minima.

In numerical simulations, we normalize the ALP field by  $\varphi \equiv \phi/\phi_{\text{in}}$  with the initial field value  $\phi_{\text{in}}$ , and parameterize the asymmetric potential by

$$\begin{aligned} V(\varphi) &= \frac{m_\phi^2 \phi_{\text{in}}^2}{2} (\varphi^2 + c_3 \varphi^3 + c_4 \varphi^4) \\ &\equiv \frac{m_\phi^2 \phi_{\text{in}}^2}{2} \tilde{V}(\varphi), \end{aligned} \quad (21)$$

where  $c_3$  and  $c_4$  are dimensionless constants. This potential is approximated by a quadratic potential for  $\varphi \ll 1/c_3, 1/\sqrt{c_4}$  and a quartic potential for  $\varphi \gg 1/c_3, 1/\sqrt{c_4}$ . In the intermediate region, the shape of the potential can be highly distorted. In the following, we assume that  $V(\varphi)$  has a unique local minimum, which requires  $c_4 > 9c_3^2/32$ . We show the shape of the asymmetric potential for  $c_3 = 40$  and  $c_4 = 460$  in Fig. 1.

To evaluate the CMB spectra with cosmic birefringence, we assume that the energy density of the ALP is negligibly small in the epoch of interest. Then, we can deal with the background cosmology and the ALP dynamics separately. We first solve the equation of motion for the axion:

$$\ddot{\varphi} + 3H\dot{\varphi} + m_\phi^2 \frac{\partial \tilde{V}(\varphi)}{\partial \varphi} = 0, \quad (22)$$

where we use the background evolution obtained by the CMB Boltzmann solver CLASS [47] for the Hubble parameter  $H$ . We translate the solution  $\varphi(t)$  into the birefringence angle  $\beta(t)$  by fixing  $g\phi_{\text{in}}$ . Then, we obtain the CMB spectra using birefCLASS [15, 48] based on CLASS. In this work, we focus on scalar perturbations and ignore tensor perturbations.

#### A. Mass potential

Let us begin with the mass potential case,  $c_3 = c_4 = 0$ , with  $m_\phi = 10^{-26}$  eV. We show the EE spectrum in Fig. 2. Here, we set  $g\phi_{\text{in}}/2 = 326$  deg. For comparison, we also show the EE spectra without birefringence, which is slightly larger than that with birefringence. The EB spectrum is highly suppressed as  $|C_l^{EB}| < 10^{-6} C_l^{EE}$  due to the oscillating  $\beta(\eta)$ .

Using this result, we can check the validity of the analytical formula for the EE spectrum (17). We evaluate the ALP amplitude at the recombination,  $\langle\phi\rangle_*$ , by

$$\langle\phi\rangle_*^2 = \phi_{\text{in}}^2 \left( \varphi_*^2 + \frac{\dot{\varphi}_*^2}{m_\phi^2} \right), \quad (23)$$

where the subscript  $*$  denotes the quantities at  $z = z_*$ . From the numerical solution of  $\varphi$ , we obtain  $g\langle\phi\rangle_*/2 \simeq$

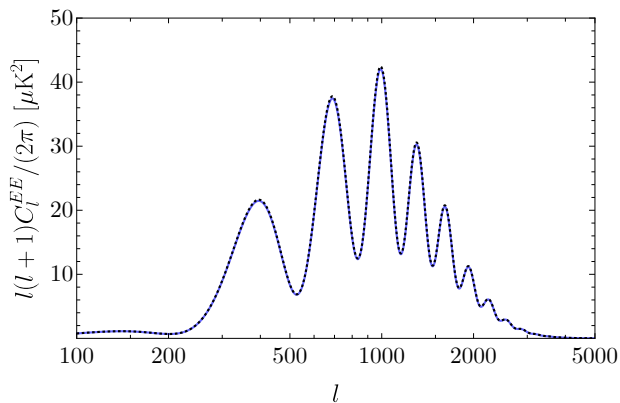


FIG. 2. EE spectrum with and without cosmic birefringence induced by the ALP with a mass potential for  $m_\phi = 10^{-26}$  eV and  $g\phi_{\text{in}}/2 = 326$  deg. The blue lines denote the spectra with birefringence, and the black-dashed lines denote the EE spectrum without birefringence. The former is slightly suppressed compared with the latter.

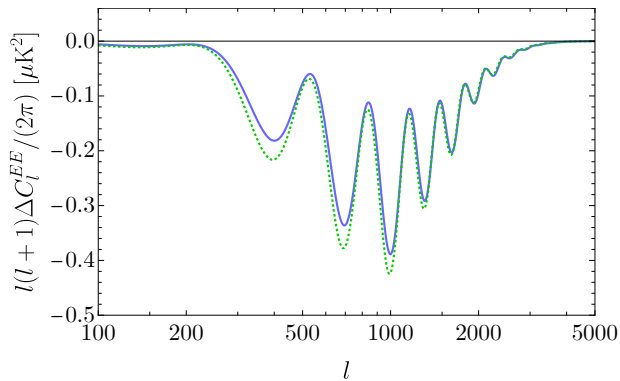


FIG. 3. Suppression of the EE spectrum due to the washout effect,  $\Delta C_l^{EE} \equiv C_l^{EE} - C_{l,0}^{EE}$ . The blue and green dashed lines denote the numerical result and analytical estimate, respectively.

$4.0^\circ \simeq 0.07$  rad. Then, we can estimate the suppressed EE spectrum as

$$C_l^{EE} \simeq 0.99 C_{l,0}^{EE}, \quad (24)$$

which saturates the upper bound from the CMB observations [30].

We show the comparison of the numerical result and analytical estimate in Fig. 3. The analytical estimate well reproduces the numerical result, and their difference is at most 10% of  $\Delta C_l^{EE} \equiv C_l^{EE} - C_{l,0}^{EE}$ . We expect that this difference comes from the time evolution of  $\langle \phi \rangle$ , which is not captured in the analytical formula. The constraints on the washout effect will be improved by a factor of 7 in terms of  $\Delta C_l^{EE}$  for the cosmic-variance limited observations [30]. Thus, the analytical formula is sufficiently accurate at least for near-future CMB observations.

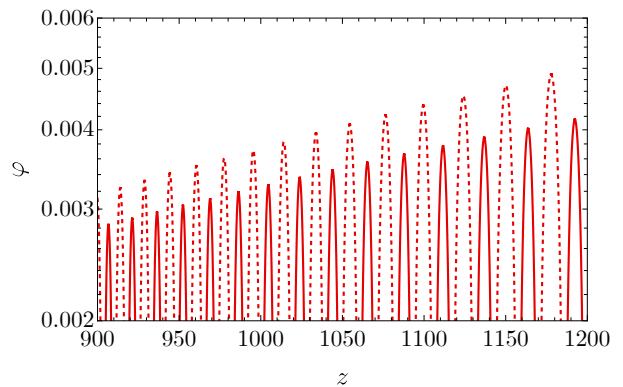


FIG. 4. Time evolution of  $\phi$  for  $m_\phi = 10^{-26}$  eV,  $c_3 = 40$ , and  $c_4 = 460$ . The solid and dashed line shows  $\phi$  and  $-\phi$ , respectively.

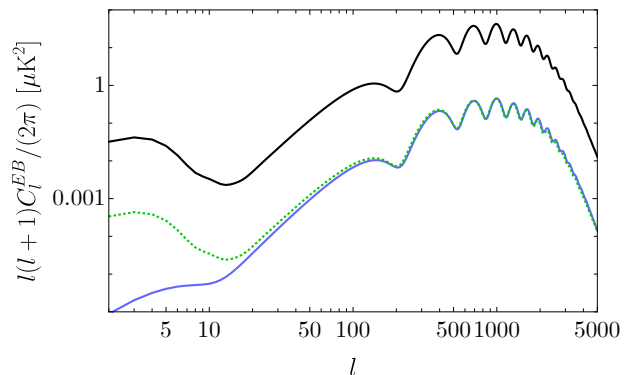


FIG. 5. EB spectrum for  $m_\phi = 10^{-26}$  eV,  $c_3 = 40$ , and  $c_4 = 460$ . The blue and green-dotted lines denote the numerical result and analytical estimate, respectively. For comparison, we also show the EE spectrum by the black line.

## B. Asymmetric potential

Next, we consider the asymmetric potential. Here, we use  $m_\phi = 10^{-26}$  eV,  $c_3 = 40$ , and  $c_4 = 460$ . We show the numerical solution for  $\phi$  in Fig. 4. Due to the distortion in the potential, the oscillation amplitudes for positive and negative  $\phi$  are different. We chose  $c_3$  and  $c_4$  so that the distortion of the potential is effective around the recombination epoch.

In this case, the EE spectrum is similar to the previous case, and the EB spectrum also becomes largely proportional to  $C_{l,0}^{EE}$  in contrast to the previous case. We show the numerical result for the EB spectra in Fig. 5. Here, we set  $g\phi_{\text{in}} = 691$  deg, which results in the EB spectrum corresponding to  $\beta = 0.3$  deg. The EB spectrum does not have the reionization bump at  $l < 10$ , which comes from linear polarization produced during the reionization epoch (see Refs. [15, 49]).

We also present analytical estimates for the EE and EB spectra. Due to the asymmetric shape of the potential, we cannot represent the oscillation of  $\phi$  by a sine

function. Here, we pick up one oscillation period from  $t_1$  to  $t_2$  around  $z = z_*$  by finding the zero points of  $\varphi(t)$ . Then, we define an effective oscillation amplitude  $\langle \phi \rangle_{*,\text{eff}}$  by

$$\langle \phi \rangle_{*,\text{eff}} \equiv \frac{\pi \phi_{\text{in}}}{2(t_2 - t_1)} \int_{t_1}^{t_2} dt |\varphi(t)|. \quad (25)$$

This definition reproduces the oscillation amplitude when  $\varphi$  oscillates following a sine function. We also obtain the averaged field value  $\bar{\phi}_*$  during the recombination epoch weighed by the visibility function as

$$\bar{\phi}_* \equiv \phi_{\text{in}} \frac{\int_{\eta_{\text{min}}}^{\eta_{\text{max}}} d\eta \tau' e^{-\tau(\eta)} \varphi(\eta)}{\int_{\eta_{\text{min}}}^{\eta_{\text{max}}} d\eta \tau' e^{-\tau(\eta)}}, \quad (26)$$

where we set  $\eta_{\text{min}}$  and  $\eta_{\text{max}}$  to the conformal time at  $z = 10^5$  and 100, respectively. Since the asymmetry of the  $\varphi$  oscillation evolves in time as well as the amplitude, we adopted the average over a long period for  $\bar{\phi}_*$  rather than the average over one period to maintain the accuracy of the approximation. Using these quantities, we estimate the spectra as

$$C_{l,\text{ana}}^{EE} = j_0^2 (g \langle \phi \rangle_{*,\text{eff}}) C_{l,0}^{EE} \simeq 0.995 C_{l,0}^{EE}, \quad (27)$$

$$C_{l,\text{ana}}^{EB} = \frac{1}{2} C_{l,0}^{EB} \sin(2g\bar{\phi}_*) \simeq 0.010 C_{l,0}^{EB}, \quad (28)$$

from the numerical solution of  $\varphi$ . While the washout effect of the EE spectrum is smaller than the current constraint, the EB spectrum reproduces  $\beta \sim 0.3$  deg, which gives  $\sin(4\beta)/2 \simeq 0.010$ . For  $l > 50$ ,  $C_{l,\text{ana}}^{EB}$  reproduces the numerical result with an accuracy of 25%.

In this example, we have obtained the EB spectrum roughly corresponding to  $\beta \sim 0.3$  deg without violating the constraint on the washout effect. Since  $\langle \phi \rangle_{*,\text{eff}}$  and  $\bar{\phi}_*$  are determined by the potential in different ways, we can obtain larger or smaller EB spectra with a fixed magnitude of the washout effect by tuning the potential parameters.

Finally, we comment on the dependence of the EB spectrum on the model parameters. To obtain a substantial EB signal, the asymmetric oscillation during the recombination epoch is essential (see Fig. 4). To realize such a situation, the quadratic, cubic, and quartic terms should contribute comparably to the potential at that time, which is not the case for general choices of  $m_\phi$ ,  $c_3$ , and  $c_4$ . If there are higher-order terms in the potential, they should not dominate over the lower-order terms during the recombination epoch to realize the asymmetric oscillation. Note that the dependence on  $\phi_{\text{in}}$  is absorbed to  $c_3$  and  $c_4$  for fixed  $m_\phi$  in our notation of the potential (21).

## IV. SUMMARY

In this paper, we investigated the effect of oscillating birefringence on the CMB polarization spectra. First, we numerically evaluated the EE and EB spectra for the mass potential and validated the analytical estimate. Then, we investigated an asymmetric potential and found that the oscillating birefringence by an asymmetric potential can explain the ICB with  $\beta \sim 0.3$  deg without violating the constraint from the washout effect. We also provided analytical formulae for the EE and EB spectra with an asymmetric potential.

Although we used  $m_\phi = 10^{-26}$  eV as an example, we have checked that the result is almost independent of  $m_\phi$  as long as  $\phi$  rapidly oscillates during the recombination epoch. Rather, the resultant EE and EB spectra are largely determined by  $\langle \phi \rangle_{*,\text{eff}}$  and  $\bar{\phi}_*$  given in Eqs. (25) and (26). Thus,  $\phi$  will be able to explain the ICB with  $\beta \sim 0.3$  deg even for  $m_\phi \gg 10^{-26}$  eV. This opens up the possibility that  $\phi$  is a significant fraction of dark matter and the origin of the ICB at the same time. Considering the X-ray constraint of  $g < 6.3 \times 10^{-13}$  GeV $^{-1}$  for the ultra-light mass region [32], we require  $\bar{\phi}_* \gtrsim 10^{10}$  GeV to obtain  $\beta \sim 0.3$  deg. Since the energy density of the ALP is at most that of dark matter, we require that  $m_\phi^2 \bar{\phi}_*^2/2$  should be smaller than the dark matter density at the recombination as a rough necessary condition. Consequently, we obtain the upper bound of  $m_\phi \lesssim 10^{-20}$  eV. This constraint becomes more severe when  $\bar{\phi}_*$  is suppressed compared to  $\langle \phi \rangle_{*,\text{eff}}$ .

In this work, we assumed that the ALP is a subdominant component in the universe and adopted a toy-model potential. To test the possibility of the ICB by ALP dark matter, we need to solve the background evolution including the ALP and the CMB spectra consistently. Since the time scale of the ALP oscillation is much shorter than that of the CMB physics, it will be computationally expensive. However, an approximate analytical solution for the evolution of  $\phi(t)$  could be used to speed up the calculations [50]. Moreover, the ALP potential should be modified for dark matter because the ALP does not behave as non-relativistic matter at the beginning of oscillations with the quartic potential. For instance, the combination of cosine-type potentials can lead to a potential distorted only in a certain region between the initial value and the potential minimum. Further detailed investigation of this possibility is left for future work.

## ACKNOWLEDGMENTS

We are grateful to Kohei Kamada, Eiichiro Komatsu, Toshiya Namikawa, Fumihito Naokawa, Ippei Obata, Maresuke Shiraishi, and Wen Yin for helpful discussions and comments. This work was supported in part by JSPS KAKENHI Grant Numbers 20H05859, 23KJ0088, and 24K17039.

- [1] Y. Minami and E. Komatsu, *New Extraction of the Cosmic Birefringence from the Planck 2018 Polarization Data*, *Phys. Rev. Lett.* **125** (2020) 221301, [2011.11254].
- [2] P. Diego-Palazuelos et al., *Cosmic Birefringence from the Planck Data Release 4*, *Phys. Rev. Lett.* **128** (2022) 091302, [2201.07682].
- [3] J. R. Eskilt, *Frequency-dependent constraints on cosmic birefringence from the LFI and HFI Planck Data Release 4*, *Astron. Astrophys.* **662** (2022) A10, [2201.13347].
- [4] J. R. Eskilt and E. Komatsu, *Improved constraints on cosmic birefringence from the WMAP and Planck cosmic microwave background polarization data*, *Phys. Rev. D* **106** (2022) 063503, [2205.13962].
- [5] COSMOGLOBE collaboration, J. R. Eskilt et al., *COSMOGLOBE DR1 results - II. Constraints on isotropic cosmic birefringence from reprocessed WMAP and Planck LFI data*, *Astron. Astrophys.* **679** (2023) A144, [2305.02268].
- [6] E. Komatsu, *New physics from the polarized light of the cosmic microwave background*, *Nature Rev. Phys.* **4** (2022) 452–469, [2202.13919].
- [7] Y. Nakai, R. Namba, I. Obata, Y.-C. Qiu and R. Saito, *Can we explain cosmic birefringence without a new light field beyond Standard Model?*, *JHEP* **01** (2024) 057, [2310.09152].
- [8] T. Fujita, K. Murai, H. Nakatsuka and S. Tsujikawa, *Detection of isotropic cosmic birefringence and its implications for axionlike particles including dark energy*, *Phys. Rev. D* **103** (2021) 043509, [2011.11894].
- [9] F. Takahashi and W. Yin, *Kilobyte Cosmic Birefringence from ALP Domain Walls*, *JCAP* **04** (2021) 007, [2012.11576].
- [10] L. W. H. Fung, L. Li, T. Liu, H. N. Luu, Y.-C. Qiu and S. H. H. Tye, *Axi-Higgs cosmology*, *JCAP* **08** (2021) 057, [2102.11257].
- [11] S. Nakagawa, F. Takahashi and M. Yamada, *Cosmic Birefringence Triggered by Dark Matter Domination*, *Phys. Rev. Lett.* **127** (2021) 181103, [2103.08153].
- [12] M. Jain, A. J. Long and M. A. Amin, *CMB birefringence from ultralight-axion string networks*, *JCAP* **05** (2021) 055, [2103.10962].
- [13] G. Choi, W. Lin, L. Visinelli and T. T. Yanagida, *Cosmic birefringence and electroweak axion dark energy*, *Phys. Rev. D* **104** (2021) L101302, [2106.12602].
- [14] I. Obata, *Implications of the cosmic birefringence measurement for the axion dark matter search*, *JCAP* **09** (2022) 062, [2108.02150].
- [15] H. Nakatsuka, T. Namikawa and E. Komatsu, *Is cosmic birefringence due to dark energy or dark matter? A tomographic approach*, *Phys. Rev. D* **105** (2022) 123509, [2203.08560].
- [16] W. Lin and T. T. Yanagida, *Consistency of the string inspired electroweak axion with cosmic birefringence*, *Phys. Rev. D* **107** (2023) L021302, [2208.06843].
- [17] S. Gasparotto and I. Obata, *Cosmic birefringence from monodromic axion dark energy*, *JCAP* **08** (2022) 025, [2203.09409].
- [18] N. Lee, S. C. Hotinli and M. Kamionkowski, *Probing cosmic birefringence with polarized Sunyaev-Zel'dovich tomography*, *Phys. Rev. D* **106** (2022) 083518, [2207.05687].
- [19] M. Jain, R. Hagimoto, A. J. Long and M. A. Amin, *Searching for axion-like particles through CMB birefringence from string-wall networks*, *JCAP* **10** (2022) 090, [2208.08391].
- [20] K. Murai, F. Naokawa, T. Namikawa and E. Komatsu, *Isotropic cosmic birefringence from early dark energy*, *Phys. Rev. D* **107** (2023) L041302, [2209.07804].
- [21] D. Gonzalez, N. Kitajima, F. Takahashi and W. Yin, *Stability of domain wall network with initial inflationary fluctuations and its implications for cosmic birefringence*, *Phys. Lett. B* **843** (2023) 137990, [2211.06849].
- [22] Y.-C. Qiu, J.-W. Wang and T. T. Yanagida, *High-Quality Axions in a Class of Chiral  $U(1)$  Gauge Theories*, *Phys. Rev. Lett.* **131** (2023) 071802, [2301.02345].
- [23] J. R. Eskilt, L. Herold, E. Komatsu, K. Murai, T. Namikawa and F. Naokawa, *Constraints on Early Dark Energy from Isotropic Cosmic Birefringence*, *Phys. Rev. Lett.* **131** (2023) 121001, [2303.15369].
- [24] T. Namikawa and I. Obata, *Cosmic birefringence tomography with polarized Sunyaev-Zel'dovich effect*, *Phys. Rev. D* **108** (2023) 083510, [2306.08875].
- [25] S. Gasparotto and E. I. Sfakianakis, *Cosmic birefringence from the Axiverse*, *JCAP* **11** (2023) 017, [2306.16355].
- [26] R. Z. Ferreira, S. Gasparotto, T. Hiramatsu, I. Obata and O. Pujolas, *Axionic defects in the CMB: birefringence and gravitational waves*, *JCAP* **05** (2024) 066, [2312.14104].
- [27] A. Greco, N. Bartolo and A. Gruppuso, *A New Solution for the Observed Isotropic Cosmic Birefringence Angle and its Implications for the Anisotropic Counterpart through a Boltzmann Approach*, **2401.07079**.
- [28] T. Fujita, Y. Minami, K. Murai and H. Nakatsuka, *Probing axionlike particles via cosmic microwave background polarization*, *Phys. Rev. D* **103** (2021) 063508, [2008.02473].
- [29] F. Finelli and M. Galaverni, *Rotation of Linear Polarization Plane and Circular Polarization from Cosmological Pseudo-Scalar Fields*, *Phys. Rev. D* **79** (2009) 063002, [0802.4210].
- [30] M. A. Fedderke, P. W. Graham and S. Rajendran, *Axion Dark Matter Detection with CMB Polarization*, *Phys. Rev. D* **100** (2019) 015040, [1903.02666].
- [31] POLARBEAR collaboration, S. Adachi et al., *Exploration of the polarization angle variability of the Crab Nebula with POLARBEAR and its application to the search for axion-like particles*, **2403.02096**.
- [32] J. S. Reynés, J. H. Matthews, C. S. Reynolds, H. R. Russell, R. N. Smith and M. C. D. Marsh, *New constraints on light axion-like particles using Chandra transmission grating spectroscopy of the powerful cluster-hosted quasar H1821+643*, *Mon. Not. Roy. Astron. Soc.* **510** (2021) 1264–1277, [2109.03261].
- [33] SPT-3G collaboration, K. R. Ferguson et al., *Searching for axionlike time-dependent cosmic birefringence with data from SPT-3G*, *Phys. Rev. D* **106** (2022) 042011, [2203.16567].
- [34] V. Iršič, M. Viel, M. G. Haehnelt, J. S. Bolton and

- G. D. Becker, *First constraints on fuzzy dark matter from Lyman- $\alpha$  forest data and hydrodynamical simulations*, *Phys. Rev. Lett.* **119** (2017) 031302, [[1703.04683](#)].
- [35] DES collaboration, E. O. Nadler et al., *Milky Way Satellite Census. III. Constraints on Dark Matter Properties from Observations of Milky Way Satellite Galaxies*, *Phys. Rev. Lett.* **126** (2021) 091101, [[2008.00022](#)].
- [36] S. M. Carroll, G. B. Field and R. Jackiw, *Limits on a Lorentz and Parity Violating Modification of Electrodynamics*, *Phys. Rev. D* **41** (1990) 1231.
- [37] S. M. Carroll and G. B. Field, *The Einstein equivalence principle and the polarization of radio galaxies*, *Phys. Rev. D* **43** (1991) 3789.
- [38] D. Harari and P. Sikivie, *Effects of a Nambu-Goldstone boson on the polarization of radio galaxies and the cosmic microwave background*, *Phys. Lett. B* **289** (1992) 67–72.
- [39] G.-C. Liu, S. Lee and K.-W. Ng, *Effect on cosmic microwave background polarization of coupling of quintessence to pseudoscalar formed from the electromagnetic field and its dual*, *Phys. Rev. Lett.* **97** (2006) 161303, [[astro-ph/0606248](#)].
- [40] G. Gubitosi, M. Martinelli and L. Pagano, *Including birefringence into time evolution of CMB: current and future constraints*, *JCAP* **12** (2014) 020, [[1410.1799](#)].
- [41] S. Lee, G.-C. Liu and K.-W. Ng, *Dark Ultra-Light Scalars and Cosmic Parity Violation*, *The Universe* **4** (2016) 29–44, [[1912.12903](#)].
- [42] M. Zaldarriaga and U. Seljak, *An all sky analysis of polarization in the microwave background*, *Phys. Rev. D* **55** (1997) 1830–1840, [[astro-ph/9609170](#)].
- [43] M. Kamionkowski, A. Kosowsky and A. Stebbins, *Statistics of cosmic microwave background polarization*, *Phys. Rev. D* **55** (1997) 7368–7388, [[astro-ph/9611125](#)].
- [44] A. Lue, L.-M. Wang and M. Kamionkowski, *Cosmological signature of new parity violating interactions*, *Phys. Rev. Lett.* **83** (1999) 1506–1509, [[astro-ph/9812088](#)].
- [45] B. Feng, H. Li, M.-z. Li and X.-m. Zhang, *Gravitational leptogenesis and its signatures in CMB*, *Phys. Lett. B* **620** (2005) 27–32, [[hep-ph/0406269](#)].
- [46] L. McAllister, E. Silverstein and A. Westphal, *Gravity Waves and Linear Inflation from Axion Monodromy*, *Phys. Rev. D* **82** (2010) 046003, [[0808.0706](#)].
- [47] J. Lesgourgues, *The Cosmic Linear Anisotropy Solving System (CLASS) I: Overview*, **1104.2932**.
- [48] F. Naokawa and T. Namikawa, *Gravitational lensing effect on cosmic birefringence*, *Phys. Rev. D* **108** (2023) 063525, [[2305.13976](#)].
- [49] B. D. Sherwin and T. Namikawa, *Cosmic birefringence tomography and calibration independence with reionization signals in the CMB*, *Mon. Not. Roy. Astron. Soc.* **520** (2023) 3298–3304, [[2108.09287](#)].
- [50] M. Galaverni, F. Finelli and D. Paoletti, *Redshift evolution of cosmic birefringence in CMB anisotropies*, *Phys. Rev. D* **107** (2023) 083529, [[2301.07971](#)].